

Self-Supervised Time-to-Event Modeling with Structured Medical Records

Ethan Steinberg, Yizhe Xu, Jason Fries, Nigam Shah

January 8, 2023

Abstract

Time-to-event models (also known as survival models) are used in medicine and other fields for estimating the probability distribution of the time until a particular event occurs. While providing many advantages over traditional classification models, such as naturally handling censoring, time-to-event models require more parameters and are challenging to learn in settings with limited labeled training data. High censoring rates, common in events with long time horizons, further limit available training data and exacerbate the risk of overfitting. Existing methods, such as proportional hazard or accelerated failure time-based approaches, employ distributional assumptions to reduce parameter size, but they are vulnerable to model misspecification. In this work, we address these challenges with MOTOR a self-supervised model that leverages temporal structure found in large-scale collections of timestamped, but largely unlabeled events, typical of electronic health record data. MOTOR defines a time-to-event pretraining task that naturally captures the probability distribution of event times, making it well-suited to applications in medicine. After pretraining on 8,192 tasks auto-generated from 2.7M patients (2.4B clinical events), we evaluate the performance of our pretrained model after fine-tuning to unseen time-to-event tasks. MOTOR-derived models improve upon current state-of-the-art C statistic performance by 6.6% and decrease training time (in wall time) by up to 8.2 times. We further improve sample efficiency, with adapted models matching current state-of-the-art performance using 95% less training data.

Keywords— time-to-event, survival, deep learning, self-supervised learning, transfer learning, foundation models

1 Introduction

Time-to-event models (which are also called *survival models*) are used for estimating the probability distribution of the time elapsed until a particular event occurs given a set of features. Time-to-event models have two primary advantages over traditional classification approaches. First, they can estimate quantities of interest, such as the hazard rate at a particular time or the median time until an event, that are difficult or impossible to compute in other approaches. Second, time-to-event models account for various types of censoring induced by different data collection mechanisms. Adjusting for censoring is critical for obtaining unbiased estimates, which in turn is important for creating fair models [Chang et al., 2022]. As a healthcare example, the 2013 ACC/AHA pooled cohort equations are used to identify patients at high risk of atherosclerotic cardiovascular disease in 10 years and determine the appropriate statin prescription [Goff et al., 2014]. In non-clinical settings, time-to-event models are used for churn prediction [Perianez et al., 2016], real time advertisement bidding [Wu et al., 2015], recommendation systems [Jing and Smola, 2017], and other business analytics.

Despite the benefits of time-to-event models, they come with a significant downside of requiring large training sets to estimate the entire time-to-event probability distribution, i.e., the probability of the event happening at every time point rather than at a single time point. A variety of methods have been proposed to mitigate this issue, generally by adding assumptions about the time-to-event distribution. These assumptions, such as proportional hazards [Cox, 1972] or parametric distributions [Martinsson, 2016, Avati et al., 2020], significantly reduce the number of parameters necessary to learn a time-to-event model, but may also degrade predictive performance when the assumptions do not hold. Regardless of these techniques,

learning higher-order interactions between features in high-dimensional datasets is challenging with limited uncensored labels.

Recent work in deep learning has approached the challenge of limited training data by relying on transfer learning via increasingly powerful *foundation models* [Bommasani et al., 2021]. Foundation models leverage advances in self-supervised learning to train models using large collections of unlabeled data. The resulting pretrained models learn broadly useful features that can then be rapidly adapted to new tasks via fine-tuning, substantially lowering the amount of labeled data and time required to train new models. Self-supervised learning requires designing a pretraining task that captures generally useful patterns in unlabeled data, typically by predicting intrinsic properties of the data itself. For example, autoregressive pretraining in NLP predicts the next word in a sequence conditioned on prior words [Radford et al., 2019]. In structured electronic health records (EHRs), which consist of text-like sequences of timestamped clinical events, autoregressive pretraining has also resulted in strong performance and improved sample efficiency in fine-tuned models [Steinberg et al., 2021]. However large-scale pretraining is underexplored for time-to-event modeling, with its benefits remaining unknown. Moreover, standard autoregressive pretraining disregards much of the temporal structure present in EHRs and it is unclear how these autoregressive objectives perform when used for more complex time-to-event modeling.

In this work, we introduce MOTOR (Many Outcome Time Oriented Representations), an approach for learning highly effective time-to-event models using transfer learning. We build on existing transfer learning techniques by developing a new self-supervised pretraining task designed specifically for time-to-event modeling. We then train a 100M parameter Transformer [Vaswani et al., 2017] model using a flexible piecewise exponential time-to-event modeling with our specialized pretraining task. The resulting Transformer model is then fine-tuned on arbitrary time-to-event target tasks of interest. Our main contributions are the following:

1. We introduce a self-supervised pretraining task for learning time-to-event models and demonstrate that the resulting model helps us train significantly better time-to-event models than state-of-the-art approaches with an average improvement in C statistic of 6.6% across several tasks.
2. We explain how to implement models that learn our time-to-event pretraining task through large-scale piecewise exponential models in a parameter efficient manner, by recognizing that these models can share time-dependent risk factors between tasks.
3. We evaluate several properties of MOTOR, including the choice of pretraining task, sample efficiency, and compute requirements. We find that time-to-event pretraining outperforms a more commonly used autoregressive pretraining objective in EHR data. We also find that fine-tuned MOTOR matches performance of state-of-the-art methods while using 95% as less training data. Finally, fine-tuning reduces training time with large datasets by up to 8.2 times (in wall time) over Random Survival Forest.

2 Related Work

2.1 Time-to-event Models

Accelerated failure time (AFT) models are a fully parametric approach for modeling time-to-event outcomes where the time-to-event distribution is parameterized with a specified probability distribution. AFT models assume that the joint effect of features is to accelerate or decelerate the time to an event by some constant, in which the effect of features is learned by optimizing a loss function, e.g., negative log-likelihood function. Common probability distributions include exponential, gamma, log-normal, log-logistic, and Weibull. To allow for additional flexibility, piecewise distributions that enable the use of different distribution parameters across different regions of time can be used, with the piecewise exponential distribution [Friedman, 1982] being a distinctly popular choice. More recently, AFT models have been combined with deep learning by using a neural network to map between input features and the parameters of specified distributions [Fornili et al., 2014, Martinsson, 2016, Ren et al., 2018, Kopper et al., 2020, Avati et al., 2020].

Cox PH models [Cox, 1972] are another common approach for time-to-event modeling that reduce the complexity of the model space by assuming a constant hazard ratio between instances over time. In situations where the proportional hazards (PH) assumption does not hold, Cox PH models may perform poorly. Similarly to AFT models, Cox models can also be combined with deep learning by using a neural network to map between the input features and the learned constant hazard ratio [Katzman et al., 2018].

Random Survival Forests (RSFs) [Ishwaran et al., 2008a] are a nonparametric approach for time-to-event modeling that works by extending random forests [Breiman, 2001] to time-to-event tasks. RSFs estimate cumulative hazard functions using the Nelson-Aalen estimator. The best splitting variable at each node is selected to maximize the survival differences between the two daughter nodes. Similar to random forests, RSFs apply bagging, random subsampling, and random variable selection techniques to improve model performance. Moreover, RSFs automatically identify nonlinear relationships among variables via the recursively partitioning scheme. Athey et al. [2019] further introduces “honest” trees for building RSFs to mitigate overfitting in which separate data sets are used for tree construction and prediction. One major limitation of RSFs is that they are computationally inefficient when applied to large-scale data [Rasmy et al., 2021a].

There has also been some work exploring how to use multi-task learning to better fit time-to-event models in cases with limited data. Li et al. [2016] proposed treating the time bins in piecewise time-to-event models as instances of related tasks and explicitly regularizing models to share weights across time bins. Gao and Cui [2022] explored using explicitly chosen “compatible” clinical tasks (i.e. clinical tasks with similar risk structure) to better learn neural network featurized Cox models. Wang and Sun [2021] evaluated learning mortality and length of stay time-to-event models simultaneously while training cancer time-to-event models. MOTOR differs from these prior approaches by focusing on scaling up the number of auxiliary tasks dramatically (up to 8,192 tasks) as part of its pretraining process.

2.2 Deep Learning For Structured EHR Data

There is a wide variety of work applying deep learning to structured Electronic Health Records (EHR) data to train models for answering complex medical questions. Early approaches, best exemplified by DeepPatient [Miotto et al., 2016] and the feedforward model in Rajkomar et al. [2018], were analogous to bag-of-words featurization from NLP and required transforming patient EHR data into sparse, count-based feature matrices where each column represents the number of times a particular medical concept occurred within a patient’s record. While this approach is parameter efficient, it requires making additional, often non-obvious, feature engineering choices to capture temporal information about events.

Recent deep learning architectures have focused on directly incorporating the temporal structure of EHR data by using either recurrent neural networks (RNNs) or attention based models such as Transformers. These time-oriented neural network models take sequential EHR data as input and model interactions between events over time. Both standard neural network architectures and EHR specific neural network architectures have been proposed for the EHR setting such as GRU-D [Che et al., 2016], RETAIN [Choi et al., 2016a], and the Transformer-based BEHRT [Li et al., 2019].

While older deep learning methods for EHR data focused on training models end-to-end using small patient cohorts, recent methods increasingly use self-supervised learning to pretrain models using millions of patient records. The resulting foundation models [Bommasani et al., 2021] demonstrate strong transfer learning properties and better performance in limited data settings via fine-tuning and other adaptation techniques. Various self-supervised objectives have been proposed for learning meaningful patterns in EHR data. DeepPatient [Miotto et al., 2016] used a denoising autoencoder objective to learn effective feedforward models. Recent approaches use objectives informed by language modeling in NLP. CLMBR [Steinberg et al., 2021] proposed an autoregressive, “next day” code prediction task to train RNN models. Many authors have presented work using masked language modeling objectives to predict masked or “corrupted” tokens in an input stream [Li et al., 2019, Rasmy et al., 2021b, Pang et al., 2021, Zeng et al., 2022].

Prior EHR deep learning models have largely focused on traditional classification tasks, however, there have been several efforts in combining deep learning with time-to-event modeling on EHR data. Avati et al. [2020] uses both RNNs and feedforward neural networks to power AFT models for estimating each patient’s time until death. Rasmy et al. [2021a] uses RNNs as a backbone for training Cox models that predict hospital mortality and ventilation needs. Wen et al. [2022] uses feedforward networks to parameterize Cox

and DeepHIT [Ryu et al., 2020] models for predicting time until discharge. MOTOR differs from this prior work in two respects. First, we generally use larger and more flexible Transformer based piecewise exponential models that can handle more complex interactions. Second, in order to handle the corresponding increase in parameters, we focus on the benefits of pretraining at a massive scale.

3 Methods

3.1 Problem Setup

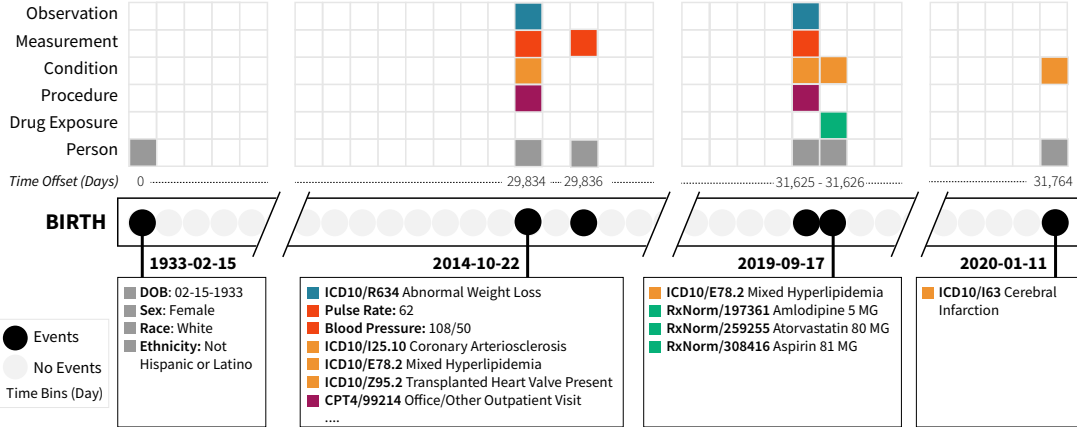


Figure 1: An example electronic health record (EHR) structured using the Observational Medical Outcomes Partnership (OMOP) Common Data Model. Each circle represents a day containing 1 or more clinical events (black) or no events (grey). Events correspond to different medical codes, color-coded by OMOP category, with examples labeled in the bottom boxes.

We consider a set of N patients and their EHRs X , where X_i denotes all information for patient i . Patient X_i consists of a sequence of timestamped clinical *events*, broadly defined as any action recorded in an EHR using a medical code. Codes are symbols drawn from a finite vocabulary defined by 26 different medical ontologies specified by our EHR data provider. For example, many EHRs use ICD10 codes [Organization, 2004] to indicate diseases, CPT codes [Dotson, 2013] to indicate procedures, RxNorm codes [Nelson et al., 2011] to indicate drugs and so forth. Let X_{ij} denote the j -th event in the sequence, where each event consists of a code for that event and the corresponding timestamp for when that event occurs. Timestamps may occur at minute or day-level resolution and can co-occur with other events. In this work, we only consider coded data and discard clinical notes and other unstructured data.

Figure 1 gives an example EHR record to demonstrate the general temporal structure of patient data. The x-axis shows the patient timeline that is offset by date of birth. On day 0, we record the patient characteristics (e.g., sex, race, and ethnicity). As time progresses, on day 29834, we observe lab measurements (e.g., pulse rate and blood pressure), medical procedures (e.g., CPT4/99214 Office/Other Outpatient Visit), and diagnosis (e.g., ICD10/I25.10 Coronary Arteriosclerosis); on day 31626, we obtain information on clinical drugs (e.g., RxNorm /197361 Amlodipine 5 MG).

We are interested in learning models to predict time-to-event tasks for patients in our dataset. For each patient i , let T_i and C_i denote the time to an event of interest and censoring time, respectively. $U_i = \min(T_i, C_i)$ is the observed follow-up time, and $\delta_i = \mathbb{1}\{T_i \leq C_i\}$ is the event indicator, which is 1 if the patient experiences the event at U_i or 0 if the patient is censored at U_i . Our estimand of interest is

$$\mathbb{P}(t|X_i) = \mathbb{P}(T_i = t), \quad (1)$$

where t is an arbitrary prediction time.

3.2 MOTOR

We introduce MOTOR, a Transformer-based neural network model that is pretrained using a self-supervised, time-to-event objective defined using structured EHR data. Figure 2 provides an overview of the overall approach, with patient records being fed into a Transformer backbone to convert them into latent representations that are then used for time-to-event pretraining predictions. The resulting pretrained MOTOR model is then combined with a linear head to train downstream, time-to-event models.

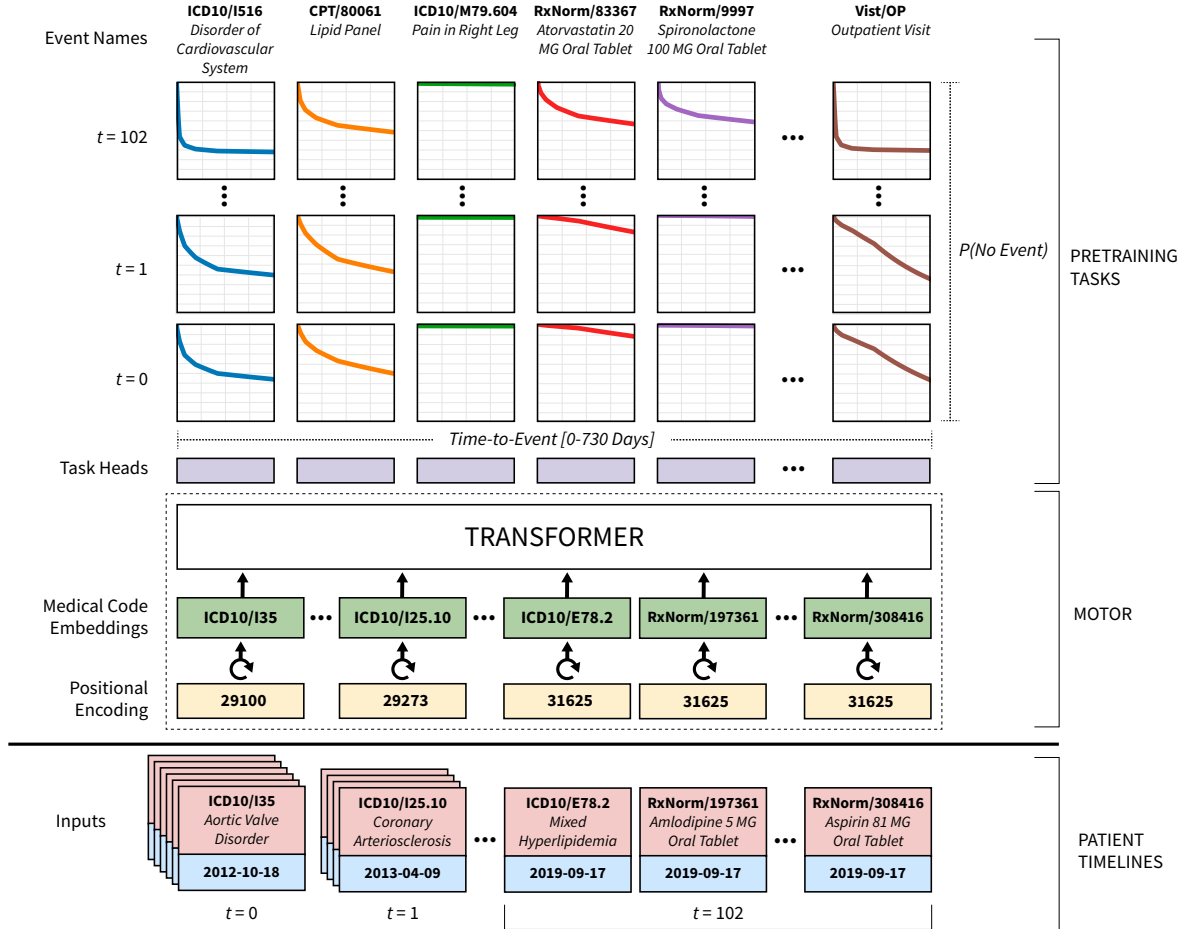


Figure 2: An overview of the MOTOR neural network architecture and the time-to-event task used for pretraining.

3.2.1 Transformer

Following the previous work of BEHRT [Li et al., 2019], we use a Transformer based neural network for processing our EHR data. X_i , the sequence of codes and timestamps for a patient i , is first transformed into a combination of code embeddings and time embeddings. Code embeddings are generated with a standard embedding layer with a vocab size of 65,536 (the maximum number of token ids that can fit in a 16 bit integer). Time embeddings are generated using a standard sinusoidal position embedding with time (in days since birth) instead of the position index being fed to the sine and cosine functions. These embeddings are then input into a Transformer to generate representations for every patient and every event in each patient’s record. The overall Transformer backbone contains 100M trainable parameters.

Our Transformer has four major changes that distinguish it from Transformer architectures commonly used with structured EHR data. First, unlike BEHRT which uses a masked language modeling objective that

incorporates bidirectional information from patient sequences, we use causally masked attention [Dai and Le, 2015, Peters et al., 2018, Raffel et al., 2022]. This attention pattern ensures information only flows forwards in the sequence and not backwards to guarantee that the model does not “cheat” by using information from the future to predict the past. If fully connected attention is used instead, models quickly learn shortcuts based on future information which causes issues when applying the model in the standard case when future data is not available. Second, we use rotary position embeddings [Su et al., 2021] for combining the time and code embeddings at every attention subunit in the network. Third, due to the long sequence lengths in our data, we use a local attention mechanism, where attention is limited to 512 token context windows, in order to avoid quadratic complexity [Roy et al., 2021]. This enables us to use sequence lengths up to 16,384 events (the maximum we can fit in 32 GB of GPU memory). Fourth, we do not use the explicit visit parts of BEHRT (the segment and position features) as our source EHR data contains overlapping visits, which is not compatible with BEHRT’s approach. Instead, we represent visits as additional clinical events within the timeline.

The output of our model is one matrix per patient R_i , where each row R_{ij} corresponds to the patient i ’s representation for the event j that contains cumulative information up to and including event j . The width of the row R_{ij} is the size of the patient representation, which is a tunable hyperparameter.

3.2.2 Piecewise Exponential Time-to-Event Model

We choose a modeling strategy that is amenable to large-scale deep learning in a setting with thousands of tasks and provides a differentiable objective that can support high censoring rates while being computationally efficient. Piecewise Exponential Artificial Neural Networks (PEANN) [Fornili et al., 2014], which combines neural networks with piecewise exponential models, is one such approach. Other approaches, like Cox based approaches, require at least one uncensored example in each batch, which introduces additional training complexity by requiring batch sampling strategies. Thus, we use a PEANN-style approach to construct piecewise exponential models for each task, indexed by k , with the hazards parameterized by neural networks.

Piecewise exponential time-to-event models require splitting the observed follow-up times into a fixed number of time bins B that cover the full possible range of event times from zero to positive infinity. Piecewise exponential models assume that the distribution of event times within each bin follows an exponential distribution (which is equivalent to assuming that the hazard rate is constant within each bin). Let λ_{ijkb} be the constant hazard rate for patient i after event j for task k within the time bin b . Note that the bin construction can be arbitrary, the only restriction is that it bins must start from zero and end at positive infinity. In our experiments, we select our bins by having the time points of each bin based on percentiles of the event times. This ensures that each bin contains an equal fraction ($1/B$) of the observed events. We tune the number of bins B as a hyperparameter.

With hazard λ_{ijkb} , it is then possible to define the standard maximum likelihood time-to-event loss function. Let δ_{ijkb} denote whether or not the i^{th} subject at the time of the j^{th} event has an event for the k^{th} task within the b^{th} bin, and let $U_{ijkb} = \max\{0, \min(T_{ijkb} - T_{ijk(b-1)}, U_{ijkb} - T_{ijk(b-1)})\}$ indicate the observed time in that bin. Recall the density function for exponential distribution is $f(U; \lambda) = \lambda \exp(-\lambda U)$, then the likelihood for uncensored subjects is $f(U; \lambda)$ and for censored subjects is $F^c(U; \lambda) = 1 - F(U; \lambda)$, where $F(U; \lambda) = 1 - \exp(-\lambda U)$ is the cumulative distribution function. Thus, the likelihood function is

$$L(U_{ijkb} | \lambda_{ijkb}) = \{\lambda_{ijkb} \exp(-\lambda_{ijkb} U_{ijkb})\}^{\delta_{ijkb}} \{\exp(-\lambda_{ijkb} U_{ijkb})\}^{1-\delta_{ijkb}} \quad (2)$$

Note that the likelihood function is specific to a particular patient index, day index, task index, and bin index. In order to obtain the likelihood function on the entire dataset, it is necessary to take the product over every patient, event, task and bin.

$$L(U | \lambda) = \prod_{i,j,k,b} L(U_{ijkb} | \lambda_{ijkb}) \quad (3)$$

3.2.3 Estimating the Hazard Given A Patient Representation

Given a particular patient representation, we need a method for computing the vector of hazard rates λ_{ijkb} in Equation (2). We assume that the transformation $R_{ij} \mapsto \log(\lambda_{ijkb})$ is a linear mapping of low rank, and

compute it with multiple smaller matrix multiplications to save on compute, memory, and parameter counts.

First, we transform our patient representation R_{ij} into a feature matrix X_{ijb} for modeling the hazard rates in each time bin b with a learned linear transformation. The feature matrix has an inner width of size p , which is a tuned parameter that defines the dimensionality of our per-time bin features. We can then compute $\log(\lambda_{ijbk}) = X_{ijb}\hat{\beta}_k$, where $\hat{\beta}_k$ is a vector of learned parameters with length p for a specific task k .

3.2.4 Time-to-Event Pretraining Task

Given our Transformer encoder, algorithm to compute hazard, and piecewise exponential time-to-event model specification, we define a pretraining task of predicting the time to various events defined by codes in our EHR data. To train a general time-to-event model that captures as much signal as possible, we train on as many tasks (codes) as we can comfortably fit into GPU memory, 8,192 in our setup. We select the 8,192 most informative codes as ranked by entropy, defined by Shannon’s formula [Shannon, 1948]:

$$H(\text{code}) = -\mathbb{P}(\text{code}) \log \mathbb{P}(\text{code}) - (1 - \mathbb{P}(\text{code})) \log \mathbb{P}(\text{code}), \quad (4)$$

where code is a code and $\mathbb{P}(\text{code})$ is the probability of code code occurring within a particular day.

In order to provide a more conservative measure of performance on novel time-to-event tasks, we take an additional step of explicitly removing codes for our evaluation target tasks from the set of pretraining tasks. Note that removing codes for evaluation is not strictly necessary for correctness as we are using a patient split to ensure no leakage between pretraining and evaluation.

We pretrain our model end-to-end using the negative log-likelihood derived based on Equation (2) averaging over all 8,192 codes. We train for 10 epochs using the Adam optimizer with the standard GPT2 [Radford et al., 2019] learning rate schedule. The learning rate and other hyperparameters are set through a grid search on the validation set. See Appendix 7 for the full details of our hyperparameter grid search.

3.2.5 Adapting MOTOR to Target Tasks

Given the pretrained model above, we can then train models for new target tasks of interest through the process of fine-tuning. Specifically, we estimate a new vector of parameters $\hat{\beta}_k^{\text{new}}$ by minimizing the new loss function defined by the new task. In order to increase the runtime efficiency and avoid overfitting, we only tune those new $\hat{\beta}_k^{\text{new}}$ parameters for each task and do not update any other weights. This is commonly done with other pretrained models such as BERT. The simpler setup of only training the new $\hat{\beta}_k^{\text{new}}$ parameters, as compared to full fine-tuning where all the weights are updated, also allows us to use a more sophisticated optimizer with faster convergence rates. To take advantage of this, we use a conjugate gradient optimizer when fine-tuning. In order to improve performance, we augment our conjugate gradient optimizer with an L2 penalty term and use the warm start optimization. We sweep the L2 regularization strength for each target task independently.

4 Experiments

We evaluate the effectiveness of the MOTOR method by performing experiments where we compare its overall performance to several alternative time-to-event modeling approaches and evaluate the impact of pretraining data size and fine-tuning data size on model performance.

4.1 Data and Compute

We use the 2022 release of the de-identified STAnford Research data repository (STAR) Observational Medical Outcomes Partnership (OMOP) [Observational Health Data Sciences and Informatics, 2022] clinical records dataset. STAR OMOP contains longitudinal EHR data for patients at Stanford Hospital and Stanford Children’s Hospital and contains 2,730,411 patients (2,368,208,275 clinical events) with most data occurring between 2014 and 2022. Each patient record consists of demographic information (age, sex, ethnicity) and coded clinical information including diagnosis codes, lab test orders and results, medication orders, procedures, and visits.

We process our dataset by converting all of the tables within the OMOP schema to a uniform timeline format of timestamped events, where each event is annotated with both the time and the clinical code for that event. We additionally perform some post-processing to correct several timestamp-related issues in the source data. In particular, we move billing codes to the end of visits to better reflect when those billing codes are clinically available and move all events annotated at 12:00 AM to 11:59 PM to better account for how 12:00 AM timestamps frequently represent day-level timestamps. We also adjust for events before birth by moving them to the date of birth.

In order to obtain unbiased evaluation metrics for the performance of methods, we split our data into training, validation, and test sets, containing 70%, 15% and 15% of the patients’ records, respectively. We perform our splitting by patient id such that each patient is assigned a split. The training set (1.9 million patients) is used for pretraining and fine-tuning target task time-to-event models, the validation set (0.4 million patients) is used for hyperparameter selection, and the test set (0.4 million patients) is used for out-of-sample evaluation. Every task (including both pretraining tasks and target tasks) uses the exact same data splits to ensure that there is no data leakage.

Experiments are performed in Stanford’s NERO compute environment using 24 Intel Xeon 2.70GHz CPU cores and 8 Nvidia V100 GPUs. Each pretraining and/or fine-tuning job is only assigned one V100 at a time.

4.2 Target Task Setup

From the STARR dataset, we derive six time-to-event target tasks, Celiac Disease, Heart Attack, Lupus, Nonalcoholic Fatty Liver Disease (NAFLD), Pancreatic Cancer, and Stroke. These tasks were chosen as they cover a wide spectrum of clinically interesting acute and chronic health conditions. Each time-to-event modeling task aims to predict the time to the clinical event of interest from a random visit in the patient record after the patient’s first year at Stanford Hospital. The clinical events are defined by a set of ICD codes. As noted in Section 3.2.4, we remove these ICD codes from our pretraining setup to better evaluate model performance on unseen tasks.

For each task, we define a set of cases and controls, where cases have the event in question and controls do not. As most patients do not have any of the diseases in our set of tasks, the number of controls vastly outnumbers the number of cases. This excess of controls creates issues evaluating some of the less computationally efficient baselines (e.g., Random Survival Forests), so we employ a naive subsampling strategy where 4 controls are randomly selected for every case. Note that this naive subsampling introduces a certain degree of censoring bias in that hazard rates are artificially scaled up due to the removal of censored examples. Appendix 7 provides the formula for the exact hazard rate scaling implied by our subsampling strategy. However, this does not affect our primary results as the resulting hazard rate scaling bias is shared across all methods and the primary goal of this study is to evaluate the relative performance of different modeling approaches. Since we evaluate and train all models using the same subsampling, the censoring bias affects them in a similar manner and our ranking of models’ performance should not be impacted. We considered correcting for this bias with a weighting strategy [Kohler et al., 2002, Van der Laan and Robins, 2003], but extreme weights induce unstable training. The set of ICD codes and the number of cases and controls are detailed in Table 1.

Table 1: Task setup details for six target tasks.

Task Name	ICD 10 Codes	Number of Cases	Number of Controls
Celiac Disease	K90.0	3453	13812
Heart Attack	I21.*	2815	11260
Lupus	M32.*	3274	13812
Pancreatic Cancer	C25.*	2163	8652
Nonalcoholic Fatty Liver Disease	K76.0	22013	88052
Stroke	I63.*	11855	47420

4.3 Methods under Comparison

We compare MOTOR with three state-of-the-art time-to-event modeling approaches that make different types of modeling assumptions: Cox PH [Cox, 1972], DeepSurv [Katzman et al., 2018], and Random Survival Forests [Ishwaran et al., 2008b].

Cox PH and Random Survival Forests cannot naively handle our sequential event format as they require input features to be in the form of a feature matrix. In order to run those methods on our dataset, we implement a featurization strategy to transform our timestamped event data into rows and columns that can be used for those methods. Following prior standard practice in the medical domain [OHDSI, 2019], we implement a count featurization strategy where a column is created for each event code in the source data and each value in that column corresponds to the number of times that event code appears in the patient record. We augment this featurization strategy by adding a hyperparameter for ontology expansion where you inject additional columns for higher level concepts, such as “Cancer” for “Lung Cancer”. Higher level concepts are determined using the SNOMED ontology [El-Sappagh et al., 2018], which provides relationships and groupings for coded information. This ontology expansion makes it easier to learn models in low data settings by increasing the overlap between the features available for each patient [Choi et al., 2016b].

In principle, DeepSurv can accept the same timestamped input format as MOTOR, however we observed poor performance due to overfitting of our larger parameterized model on our small time-to-event datasets. Instead, we train DeepSurv on the same feature matrices used for Random Survival Forests and Cox PH. These models are less prone to overfitting because they do not require estimating as many parameters as we can use simpler non-sequence oriented neural network models. We parameterize DeepSurv with a three layer feedforward neural network with a rectified linear unit (ReLU) activation function and batch-normalization. As in MOTOR, we use dropout and early stopping for regularization.

Appendix 7 contains the full hyperparameter search grids for all approaches as well as the software versions used when applicable.

4.4 Experiment Schema

We focus on evaluating the model performance of MOTOR, as well as the methods in Section 4.3, in the following aspects:

- a Overall Performance: We compare MOTOR with three baseline time-to-event methods using all available target task data.
- b Performance of Pretraining Task: We examine the performance of MOTOR on the pretraining task.
- c Choice of Pretraining Task: We compare our time-to-event pretraining task to an auto-regressive, next code pretraining task.
- d Sample Size Used in Pretraining: We examine the impact of pretraining on model performance by conducting pretraining on a decreasing proportion of the training data. We evaluate using 5%, 10%, and 25% of our training split for pretraining.
- e Sample Size Used in Fine-tuning: We examine the impact of the fine-tuning sample size on model performance. We use all the training samples for pretraining but randomly sample 5%, 10% and 25% of the training split for fine-tuning.
- f Time-to-Train: We compare the implementation wall time of MOTOR to that of the second most performant predictive method, Random Survival Forests.

4.5 Evaluation Metrics

We evaluate model performance using two metrics, the time-dependent C statistic and the Nam-D’Agostino (ND) calibration metric [D’Agostino and Nam, 2003]. These metrics were chosen because they can be used to evaluate time-dependent risk (which cannot be done with time-independent metrics like Harrell’s C statistic).

The time-dependent C statistic summarizes the ability of a predictive model to rank patients by risk based on their instantaneous hazard functions. Specifically, we apply the incident and dynamic definitions

for the time-dependent sensitivity and specificity, respectively, following the choices in [Heagerty and Zheng \[2005\]](#):

$$\begin{aligned}\text{sen}^{\mathbb{I}}(c, t) &= \mathbb{P}(S_i > c | dN_i^*(t) = 1) \\ \text{spe}^{\mathbb{D}}(c, t) &= \mathbb{P}(S_i \leq c | N_i^*(t) = 0),\end{aligned}$$

where S_i is the predicted risk score for subject i . $N_i^*(t) = \mathbb{1}\{T_i \leq t\}$ and $dN_i^*(t) = N_i^*(t) - N_i^*(t-)$ follow the standard definitions of a counting process. Then, the concordance can be expressed as a weighted average of the area under the time-dependent receiver operating curve (ROC)

$$C = \frac{\int_t \text{AUC}(t) w(t) dt}{\int_t w(t) dt} \quad (5)$$

where $w(t) = f(t) \cdot S(t)$. $f(t)$ is the event rate at a particular time t and $S(t)$ is the survival probability at that time. Both $f(t)$ and $S(t)$ are estimated using the Kaplan-Meier estimator. $\text{AUC}(t)$ is the time-specific area under ROC and can be computed by integration, and ROC can be calculated using $\text{sen}^{\mathbb{I}}$ and $\text{spe}^{\mathbb{D}}$ with the standard formulation.

Note that the formula in Equation (5) is slightly modified from [Heagerty and Zheng \[2005\]](#) because our dataset contains many events that happened at the exact same time due to some events having only day-level time resolution. [Heagerty and Zheng \[2005\]](#) assumes that all event times are distinct thus the sum of the weights (the term in the denominator) is $\frac{1}{2}$. As we have many tied event times, we cannot make the same assumption and have to explicitly compute the denominator as $\int_t w(t) dt$.

The ND calibration metric [[D'Agostino and Nam, 2003](#)] is constructed based on the idea that the survival probability estimates, $\hat{S}(t) = P(T_i > t)$, for a particular time t should be calibrated with respect to the number of observed survivors past that time point, which is not available in censored data, thus we estimate it using the Kaplan-Meier estimator per [D'Agostino and Nam \[2003\]](#). First, the data is sorted by $\hat{S}(t)$ given by a model and split into M equal size risk bins, where $\underline{p(t)}_m$ is the average value of $\hat{S}(t)$ within bin m . Second, a KM estimator is fit within each risk bin for computing actual survival probabilities. Finally, the squared difference between the expected and actual values is computed and summed across bins. The resulting statistic is χ^2 with $M - 1$ degrees of freedom. In principle, you can run hypotheses tests using this statistic, but we instead directly report and compare the raw statistic

$$\chi^2(t) = \sum_{m=1}^M \frac{[KM(t)_m - \overline{p(t)}_m]^2 n_m}{\underline{p(t)}_m (1 - \underline{p(t)}_m)}, \quad (6)$$

where n_m is the number of observations in bin m . For all evaluations, we set t to the median event time. In addition, we make one minor modification to this metric in that we remove the n_m term in the numerator as we are primarily concerned about relative performance. It's a constant factor that only depends on the number of patients for each task, and removing it makes it easier to compare results across target tasks.

The time-dependent C statistic and ND test become increasingly unstable as the censoring rate increases since they rely on Kaplan Meier estimators that themselves become unstable at higher censoring rates. As such, it is generally recommended to only compute these statistics on a subset of the possible times to reduce the variance of estimates. As suggested by [Heagerty and Zheng \[2005\]](#), we use the time-restricted variants of these evaluation metrics by setting a time limit of the 90% percentile of observed event times and only perform evaluations up to that time point.

In order to accurately quantify statistical significance, we use the paired test-set bootstrap approach [[Konietschke and Pauly, 2013](#)] to estimate the 95% confidence interval for the difference in model performance between MOTOR and every other method. For every target task, we resample our test set with replacement to obtain 1000 bootstrap samples. We then compute all metrics for all of our models on each bootstrap sample, subtracting MOTOR's performance each time to obtain an estimate of how each method differs from MOTOR. We finally compute confidence intervals by extracting the 2.5% and 97.5% percentiles of the bootstrapped samples. All of our confidence intervals for the differences in performance between methods are reported in Appendix 7.

5 Results

5.1 Overall Performance

Table 2 provides the time-dependent concordance performance of the various methods trained on the full dataset. MOTOR performs substantially better than all of our baselines, providing statistically significant higher C statistics in all of our six tasks (Table S2). In addition, we see approaches that make stronger assumptions show worse ranking performance under complicated data structures. The Cox model results in the lowest C statistics since it assumes both proportional hazard and a linear relationship between the log hazard and covariates. Both DeepSurv (which does not make this linear assumption) and Random Survival Forests (which is completely nonparametric) show improved C statistics.

We also report a particularly important ablation of MOTOR vs MOTOR without any pretraining (MOTOR-WP). As MOTOR combines a sophisticated neural network model with pretraining, it's important to demonstrate that pretraining itself provides value. MOTOR-WP uses the exact same piecewise exponential setup, Transformer backbone, and the hyperparameter grid as MOTOR, with the only change being that MOTOR-WP is only trained on the target tasks. MOTOR-WP performs worse than MOTOR, demonstrating the importance of pretraining for modeling time-to-event tasks.

Table 2: Time-dependent C statistic for the various methods on the full dataset. Larger values indicate better ranking performance. Bolding indicates the best performing model. RSF = Random Survival Forests. MOTOR-WP = MOTOR Without Pretraining

Method	Celiac	Heart Attack	Lupus	NAFLD	Pancreatic Cancer	Stroke
Cox PH	0.689	0.761	0.770	0.726	0.793	0.779
DeepSurv	0.704	0.823	0.790	0.800	0.811	0.830
RSF	0.729	0.836	0.787	0.802	0.824	0.840
MOTOR-WP	0.696	0.795	0.803	0.821	0.777	0.831
MOTOR	0.802	0.884	0.850	0.859	0.865	0.874

Table 3 provides the corresponding overall ND calibration results. MOTOR yields the smallest (modified) ND statistics for most of the target tasks; however, the improvements are not statistically significant given the overlapping confidence intervals in Table S3. Compared to the Cox PH model, the nonlinear DeepSurv results in smaller ND statistics but only shows statistically significant better performance for the Lupus task. Of note is that the MOTOR-WP baseline has substantially worse calibration, which is a common failure mode for neural network models [Guo et al., 2017].

Table 3: ND calibration for the various methods on the full dataset. Smaller values indicate smaller calibration errors. Bolding indicates the best performing model. RSF = Random Survival Forests. MOTOR-WP = Motor Without Pretraining.

Method	Celiac	Heart Attack	Lupus	NAFLD	Pancreatic Cancer	Stroke
Cox PH	0.167	0.214	0.373	0.121	0.141	0.031
DeepSurv	0.041	0.089	0.102	2.911	0.081	0.023
RSF	0.299	0.225	0.095	0.091	0.345	0.112
MOTOR-WP	4.970	3.990	23.882	0.077	7.104	0.083
MOTOR	0.045	0.029	0.059	0.019	0.046	0.032

5.2 Performance of Pretraining Task

When MOTOR is being pretrained, we are implicitly training 8,192 piecewise exponential time-to-event models across a variety of medical codes. Assessing pretraining performance is important because it allows us to evaluate MOTOR's performance on a wider variety of tasks with vastly different censoring rates than

our subsampled target tasks. Figure 3 provides the C statistic as a function of the amount of uncensored data for each task, with lines indicating the C statistics of the first quartile (0.783), median (0.840), and third quartile (0.898).

Performance on the pretraining tasks is strong across the vast majority of tasks, as indicated by the relatively high first quartile C statistic of 0.783. It's noteworthy that performance is strong even for highly censored tasks, even when only one in a thousand patients have an uncensored event.

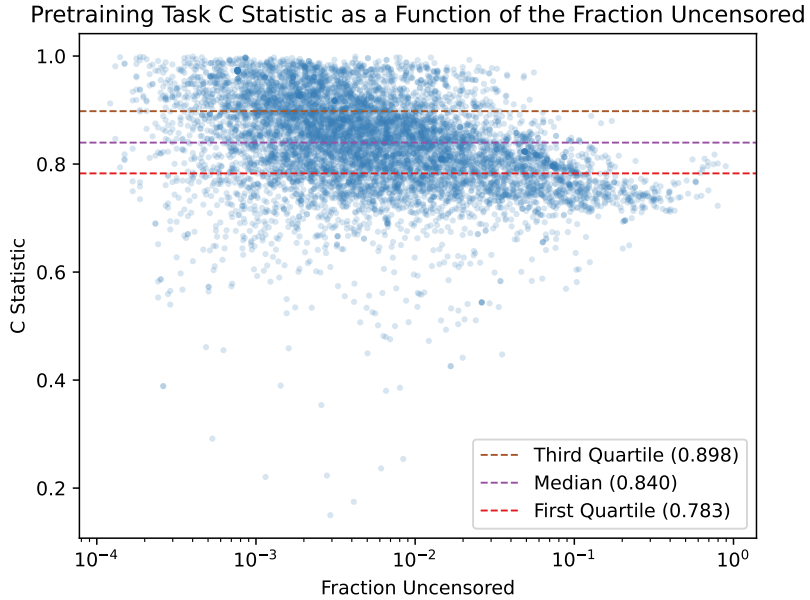


Figure 3: Pretraining task C statistic as a function of the fraction of uncensored data. The dotted lines indicate the quartiles for the C statistic across all fractions of uncensored data.

5.3 Choice of Pretraining Task

One of the main novel components of MOTOR is our time-to-event pretraining task. In order to investigate how much this pretraining task contributes to MOTOR’s performance, we perform a comparison with another common EHR pretraining task: next code prediction. This autoregressive pretraining task aims to predict the next code in an EHR sequence [Steinberg et al., 2021]. One limitation of the next code prediction setup is that we are unable to perform a straightforward linear head fine-tuning step because the next code prediction pretraining task does not contain the necessary linear transformation from R_{ij} to X_{ijb} in our piecewise exponential model.

Instead, for this experiment, we perform full weight updates while fine-tuning, updating every weight in the model using gradient descent. In order to ensure a fair comparison, we apply the same tweak to MOTOR and then compare performance on our target tasks. We thus ensure that both pretraining tasks have a matched setup, with the same architecture, hyperparameter search grid, and fine-tuning strategy.

Table 4 compares the next code pretraining task to our time-to-event pretraining task. We see that the time-to-event pretraining task outperforms the next code pretraining task, indicated by the statistically significant higher C statistics on most of the target tasks (Table S4). This implies that utilizing a time-to-event pretraining task is beneficial for predicting time-to-event outcomes.

5.4 Sample Size Used in Pretraining

As MOTOR relies on pretraining to achieve good performance, an important question is how MOTOR’s performance changes as a function of available pretraining data. We evaluate 5% to 25% uniform random

Table 4: Impact of the pretraining objective on the performance of MOTOR in terms of the time-dependent C statistic. We compare a “next code” baseline with our proposed time-to-event objective. Note that these experiments are conducted with full fine-tuning of the entire model.

Objective	Celiac	Heart Attack	Lupus	NAFLD	Pancreatic Cancer	Stroke
Next Code	0.774	0.862	0.842	0.860	0.860	0.857
Time-to-Event	0.800	0.881	0.858	0.864	0.861	0.874

samples of our pretraining dataset and report performance for all target tasks. Table 5 shows that performance degrades quite rapidly as the pretraining data size decreases, quickly approaching the performance of the baselines for smaller pretraining sizes. The decreased performance of MOTOR on these subsampled datasets likely reflects overfitting that occurs when training our high-parameter model on relatively small time-to-event datasets.

Table 5: Impact of pretraining on the performance of MOTOR in terms of the time-dependent C statistic. We utilize a subset of the full training data to conduct pretraining. K = thousand patients. M = million patients.

# Patients For Pretraining	Celiac	Heart Attack	Lupus	NAFLD	Pancreatic Cancer	Stroke
95K (5%)	0.694	0.843	0.740	0.768	0.825	0.824
191K (10%)	0.714	0.849	0.749	0.786	0.831	0.828
478K (25%)	0.742	0.853	0.788	0.799	0.837	0.833
1.91M (100%)	0.802	0.884	0.850	0.859	0.865	0.874

5.5 Sample Size Used for Fine-tuning

A key benefit of foundation models is improved sample efficiency, enabling the adaptation of pretrained models to novel tasks while requiring fewer labeled training examples. We evaluate MOTOR’s sample efficiency by randomly subsampling the datasets for our target tasks and fine-tuning MOTOR on these smaller datasets. We evaluate on 5%, 10% and 25% and 100% of the original fine-tuning datasets.

Table 6 contains the time-dependent C statistics for each of those reduced training sets. Even though decreasing fine-tuning sample sizes induces lower C statistics (Table S6), MOTOR still has strong ranking performance even with only 5% of the original training data for fine-tuning. This probably reflects that there are many similar tasks within the pretraining set, enabling efficient fine-tuning even given limited available task data for training.

Table 6: Impact of sample sizes for fine-tuning MOTOR on the time-dependent C statistic. We utilize a subset of the full training data to conduct pretraining. 100% corresponds to the entire training dataset.

% Used	Celiac	Heart Attack	Lupus	NAFLD	Pancreatic Cancer	Stroke
5%	0.785	0.878	0.840	0.851	0.849	0.868
10%	0.781	0.874	0.844	0.854	0.854	0.868
25%	0.790	0.880	0.845	0.856	0.859	0.869
100%	0.802	0.884	0.850	0.859	0.865	0.874

5.6 Time-to-Train

The ability to fit time-to-event models quickly is essential for a variety of scenarios such as interactive model training and limited resource environments. One of the main advantages of MOTOR is that almost all of the

weights can be frozen during fine-tuning, which means that one can learn target task models very quickly by only computing gradients for the linear heads.

In order to evaluate model training time, we perform timing experiments on all of our six target tasks, comparing MOTOR to the current state-of-the-art, Random Survival Forests. To simplify our experimental setup, we ignore the cost of hyperparameter tuning and focus solely on the time to fit the final target task models with the optimally determined hyperparameters. We provide 16 CPU cores, one V100 GPU, and 100 GB of RAM on isolated machines to both Random Survival Forests and MOTOR.

Table 7 contains the clock time, in minutes for both methods on each task. The main variable which affects the runtime is the number of patients per task, which is described in Table 1. Note that Random Survival Forests is more efficient on tasks with fewer patients, where the overhead of MOTOR is more significant. However, this completely flips for the tasks with many patients, in particular NAFLD and Stroke, where the increased efficiency of MOTOR allows us to train target task models more quickly than Random Survival Forests, with an 8.2x increase in speed for the NAFLD task. We note this is a somewhat conservative time comparison that ignores the cost and additional workflow complexity of materializing Random Survival Forests’ feature matrix.

Table 7: The time it takes to train a target task model, in minutes. Each run is given 16 CPU cores, one V100 GPU, and 100 GB of RAM. The fastest method for each target task is bolded. RSF = Random Survival Forests.

Method	Celiac	Heart Attack	Lupus	NAFLD	Pancreatic Cancer	Stroke
RSF	1.82	1.21	5.80	93.31	2.08	22.22
MOTOR	2.35	2.47	2.40	11.45	2.16	7.50

6 Discussion

We proposed a novel and effective approach, which we call MOTOR, for learning time-to-event models using transfer learning. The use of transfer learning allows MOTOR to mitigate the key issue of overfitting in standard time-to-event analysis approaches, which allows MOTOR to use more sophisticated high-parameter models even in limited data settings. From conducting a comprehensive experiment, we show that MOTOR outperforms several state-of-the-art approaches and provides estimators with strong ranking and calibration performance across a range of clinical tasks. Such success is attributed to the novel time-to-event pre-training process that enables MOTOR to learn sophisticated interactions and event distributions over 8,192 informative events.

In addition, MOTOR is scalable and computationally efficient. We only need to pretrain MOTOR once on the entire dataset, and then the same pretrained model can be reused many times on an arbitrary number of target tasks. As this fine-tuning only requires updating a small number of weights, it is very computationally efficient, allowing us to train task-specific models up to eight times faster than Random Survival Forests. The decreased computation costs of MOTOR make time-to-event models much more practical in clinical settings with limited computational resources.

This work has several limitations. First, pretraining MOTOR is quite expensive, often requiring several GPU days in our experiments. Even though this is a one-time cost, it might be prohibitive in some severely resource-constrained settings. Second, our experimental protocol performed evaluations on subsampled target task datasets to allow us to evaluate more methods. Doing so introduces a certain degree of censoring bias, which might affect our results. Third, we only evaluated MOTOR on ICD code-derived tasks to simplify the labeling effort. In some cases, assigning labels to specific medical conditions or outcomes requires developing complicated phenotyping rules and machine learning-based methods [Banda et al., 2018]. We leave evaluating MOTOR in these settings for future work.

7 Conclusion

In conclusion, we validated that MOTOR is an effective approach for learning reliable time-to-event models for a variety of tasks, even in the presence of limited data. The use of pretraining, and in particular the specialized time-to-event pretraining task, allows us to learn flexible deep neural network time-to-event models in low sample settings and low compute resource situations where they would otherwise not be viable.

Acknowledgements

This work was supported by R01 HL144555 from the National Heart, Lung, and Blood Institute (NHLBI).

References

S. Athey, J. Tibshirani, and S. Wager. Generalized random forests. *Ann. Statist.*, pages 47(2): 1148–1178, 2019.

A. Avati, T. Duan, S. Zhou, K. Jung, N. H. Shah, and A. Y. Ng. Countdown regression: sharp and calibrated survival predictions. In *Uncertainty in Artificial Intelligence*, pages 145–155. PMLR, 2020.

J. M. Banda, M. Seneviratne, T. Hernandez-Boussard, and N. H. Shah. Advances in electronic phenotyping: from rule-based definitions to machine learning models. *Annual review of biomedical data science*, 1:53, 2018.

R. Bommasani, D. A. Hudson, E. Adeli, R. Altman, S. Arora, S. von Arx, M. S. Bernstein, J. Bohg, A. Bosselut, E. Brunskill, et al. On the opportunities and risks of foundation models. *arXiv preprint arXiv:2108.07258*, 2021.

L. Breiman. Random forests. *Machine Learning*, pages 45: 5–32, 2001.

T. Chang, M. W. Sjoding, and J. Wiens. Disparate censorship & undertesting: A source of label bias in clinical machine learning, 2022. URL <https://arxiv.org/abs/2208.01127>.

Z. Che, S. Purushotham, K. Cho, D. Sontag, and Y. Liu. Recurrent neural networks for multivariate time series with missing values, 2016. URL <https://arxiv.org/abs/1606.01865>.

E. Choi, M. T. Bahadori, J. A. Kulas, A. Schuetz, W. F. Stewart, and J. Sun. Retain: An interpretable predictive model for healthcare using reverse time attention mechanism, 2016a. URL <https://arxiv.org/abs/1608.05745>.

E. Choi, M. T. Bahadori, L. Song, W. F. Stewart, and J. Sun. Gram: Graph-based attention model for healthcare representation learning, 2016b. URL <https://arxiv.org/abs/1611.07012>.

D. R. Cox. Regression models and life-tables. *Journal of the Royal Statistical Society: Series B (Methodological)*, 34(2):187–202, 1972.

R. D’Agostino and B.-H. Nam. Evaluation of the performance of survival analysis models: Discrimination and calibration measures. In *Advances in Survival Analysis*, volume 23 of *Handbook of Statistics*, pages 1–25. Elsevier, 2003. doi: [https://doi.org/10.1016/S0169-7161\(03\)23001-7](https://doi.org/10.1016/S0169-7161(03)23001-7). URL <https://www.sciencedirect.com/science/article/pii/S0169716103230017>.

A. M. Dai and Q. V. Le. Semi-supervised sequence learning. In C. Cortes, N. Lawrence, D. Lee, M. Sugiyama, and R. Garnett, editors, *Advances in Neural Information Processing Systems*, volume 28. Curran Associates, Inc., 2015. URL <https://proceedings.neurips.cc/paper/2015/file/7137debd45ae4d0ab9aa953017286b20-Paper.pdf>.

P. Dotson. Codes: What Are They, Why Are They Necessary, and How Are They Developed? *Adv Wound Care (New Rochelle)*, 2(10):583–587, Dec 2013.

S. El-Sappagh, F. Franda, F. Ali, and K. S. Kwak. SNOMED CT standard ontology based on the ontology for general medical science. *BMC Med Inform Decis Mak*, 18(1):76, Aug 2018.

M. Fornili, F. Ambrogi, P. Boracchi, and E. Biganzoli. Piecewise exponential artificial neural networks (peann) for modeling hazard function with right censored data. In E. Formenti, R. Tagliaferri, and E. Wit, editors, *Computational Intelligence Methods for Bioinformatics and Biostatistics*, pages 125–136, Cham, 2014. Springer International Publishing. ISBN 978-3-319-09042-9.

M. Friedman. Piecewise exponential models for survival data with covariates. *The Annals of Statistics*, 10(1):101–113, 1982.

Y. Gao and Y. Cui. Clinical time-to-event prediction enhanced by incorporating compatible related outcomes. *PLOS Digit Health*, 1(5), 2022.

D. Goff, D. Lloyd-Jones, G. Bennett, S. Coady, R. D’Agostino, R. Gibbons, P. Greenland, D. Lackland, D. Levy, C. O’Donnell, et al. American college of cardiology/american heart association task force on practice guidelines. 2013 acc/aha guideline on the assessment of cardiovascular risk: a report of the american college of cardiology/american heart association task force on practice guidelines. *Circulation*, 129(25 suppl 2):49–73, 2014.

C. Guo, G. Pleiss, Y. Sun, and K. Q. Weinberger. On calibration of modern neural networks. *CoRR*, abs/1706.04599, 2017. URL <http://arxiv.org/abs/1706.04599>.

P. J. Heagerty and Y. Zheng. Survival model predictive accuracy and roc curves. *Biometrics*, 61(1):92–105, 2005.

H. Ishwaran, U. Kogalur, E. Blackstone, and et al. Random survival forests. *Ann Appl Stat*, pages 2(3):841–860, 2008a.

H. Ishwaran, U. B. Kogalur, E. H. Blackstone, and M. S. Lauer. Random survival forests. *The Annals of Applied Statistics*, 2(3), sep 2008b. doi: 10.1214/08-aoas169. URL <https://doi.org/10.1214/08-aoas169>.

H. Jing and A. J. Smola. Neural survival recommender. In *Proceedings of the Tenth ACM International Conference on Web Search and Data Mining*, WSDM ’17, page 515–524, New York, NY, USA, 2017. Association for Computing Machinery. ISBN 9781450346757. doi: 10.1145/3018661.3018719. URL <https://doi.org/10.1145/3018661.3018719>.

J. L. Katzman, U. Shaham, A. Cloninger, J. Bates, T. Jiang, and Y. Kluger. DeepSurv: personalized treatment recommender system using a cox proportional hazards deep neural network. *BMC Medical Research Methodology*, 18(1), feb 2018. doi: 10.1186/s12874-018-0482-1. URL <https://doi.org/10.1186/s12874-018-0482-1>.

M. Kohler, K. Máthé, and M. Pintér. Prediction from randomly right censored data. *Journal of Multivariate Analysis*, 80(1):73–100, 2002.

F. Konietschke and M. Pauly. Bootstrapping and permuting paired t-test type statistics. *Statistics and Computing*, 24(3):283–296, Jan. 2013. doi: 10.1007/s11222-012-9370-4. URL <https://doi.org/10.1007/s11222-012-9370-4>.

P. Kopper, S. Pölsterl, C. Wachinger, B. Bischl, A. Bender, and D. Rügamer. Semi-structured deep piecewise exponential models. *CoRR*, abs/2011.05824, 2020. URL <https://arxiv.org/abs/2011.05824>.

Y. Li, J. Wang, J. Ye, and C. K. Reddy. A multi-task learning formulation for survival analysis. In *Proceedings of the 22nd ACM SIGKDD International Conference on Knowledge Discovery and Data Mining*, KDD ’16, page 1715–1724, New York, NY, USA, 2016. Association for Computing Machinery. ISBN 9781450342322. doi: 10.1145/2939672.2939857. URL <https://doi.org/10.1145/2939672.2939857>.

Y. Li, S. Rao, J. R. A. Solares, A. Hassaine, D. Canoy, Y. Zhu, K. Rahimi, and G. Salimi-Khorshidi. Behrt: Transformer for electronic health records, 2019. URL <https://arxiv.org/abs/1907.09538>.

E. Martinsson. *Wtte-rnn: Weibull time to event recurrent neural network*. PhD thesis, Chalmers University of Technology & University of Gothenburg, 2016.

R. Miotto, L. Li, B. A. Kidd, and J. T. Dudley. Deep Patient: An Unsupervised Representation to Predict the Future of Patients from the Electronic Health Records. *Sci Rep*, 6:26094, May 2016.

S. J. Nelson, K. Zeng, J. Kilbourne, T. Powell, and R. Moore. Normalized names for clinical drugs: RxNorm at 6 years. *J Am Med Inform Assoc*, 18(4):441–448, 2011.

Observational Health Data Sciences and Informatics. Omop common data model. <https://ohdsi.github.io/CommonDataModel/index.html>, 2022.

OHDSI. *The Book of OHDSI: Observational Health Data Sciences and Informatics*. OHDSI, 2019. ISBN 9781088855195. URL <https://books.google.com/books?id=JxpnzQEACAAJ>.

W. H. Organization. Icd-10 : international statistical classification of diseases and related health problems : tenth revision, 2004.

C. Pang, X. Jiang, K. S. Kalluri, M. Spotnitz, R. Chen, A. Perotte, and K. Natarajan. Cehr-bert: Incorporating temporal information from structured ehr data to improve prediction tasks. In S. Roy, S. Pfohl, E. Rocheteau, G. A. Tadesse, L. Oala, F. Falck, Y. Zhou, L. Shen, G. Zamzmi, P. Mugambi, A. Zirikly, M. B. A. McDermott, and E. Alsentzer, editors, *Proceedings of Machine Learning for Health*, volume 158 of *Proceedings of Machine Learning Research*, pages 239–260. PMLR, 04 Dec 2021. URL <https://proceedings.mlr.press/v158/pang21a.html>.

A. Perianez, A. Saas, A. Guitart, and C. Magne. Churn prediction in mobile social games: Towards a complete assessment using survival ensembles. In *2016 IEEE International Conference on Data Science and Advanced Analytics (DSAA)*. IEEE, oct 2016. doi: 10.1109/dsaa.2016.84. URL <https://doi.org/10.1109%2Fdsaa.2016.84>.

M. E. Peters, M. Neumann, M. Iyyer, M. Gardner, C. Clark, K. Lee, and L. Zettlemoyer. Deep contextualized word representations. In *Proceedings of the 2018 Conference of the North American Chapter of the Association for Computational Linguistics: Human Language Technologies, Volume 1 (Long Papers)*, pages 2227–2237, New Orleans, Louisiana, June 2018. Association for Computational Linguistics. doi: 10.18653/v1/N18-1202. URL <https://aclanthology.org/N18-1202>.

A. Radford, J. Wu, R. Child, D. Luan, D. Amodei, and I. Sutskever. Language models are unsupervised multitask learners. 2019.

C. Raffel, N. Shazeer, A. Roberts, K. Lee, S. Narang, M. Matena, Y. Zhou, W. Li, and P. J. Liu. Exploring the limits of transfer learning with a unified text-to-text transformer. *J. Mach. Learn. Res.*, 21(1), jun 2022. ISSN 1532-4435.

A. R. Rajkomar, E. Oren, K. Chen, A. Dai, N. Hajaj, M. Hardt, P. J. Liu, X. Liu, J. Marcus, M. Sun, P. P. Sundberg, H. Yee, K. Zhang, Y. Zhang, G. Flores, G. Duggan, J. Irvine, Q. Le, K. Litsch, A. Mossin, J. J. Tansuwan, D. Wang, J. Wexler, J. Wilson, D. Ludwig, S. Volchenboum, K. Chou, M. Pearson, S. Madabushi, N. Shah, A. Butte, M. Howell, C. Cui, G. Corrado, and J. Dean. Scalable and accurate deep learning for electronic health records. *npj Digital Medicine*, 2018. URL <https://www.nature.com/articles/s41746-018-0029-1>.

L. Rasmy, M. Nigo, B. S. Kannadath, Z. Xie, B. Mao, K. Patel, Y. Zhou, W. Zhang, A. Ross, H. Xu, and D. Zhi. Covrnn—a recurrent neural network model for predicting outcomes of covid-19 patients: model development and validation using ehr data. *medRxiv*, 2021a. doi: 10.1101/2021.09.27.21264121. URL <https://www.medrxiv.org/content/early/2021/09/29/2021.09.27.21264121>.

L. Rasmy, Y. Xiang, Z. Xie, C. Tao, and D. Zhi. Med-BERT: pretrained contextualized embeddings on large-scale structured electronic health records for disease prediction. *npj Digital Medicine*, 4(1), May 2021b. doi: 10.1038/s41746-021-00455-y. URL <https://doi.org/10.1038/s41746-021-00455-y>.

K. Ren, J. Qin, L. Zheng, Z. Yang, W. Zhang, L. Qiu, and Y. Yu. Deep recurrent survival analysis, 2018. URL <https://arxiv.org/abs/1809.02403>.

A. Roy, M. Saffar, A. Vaswani, and D. Grangier. Efficient content-based sparse attention with routing transformers. *Transactions of the Association for Computational Linguistics*, 9:53–68, 2021. doi: 10.1162/tacl_a_00353. URL <https://aclanthology.org/2021.tacl-1.4>.

J. Y. Ryu, M. Y. Lee, J. H. Lee, B. H. Lee, and K. S. Oh. DeepHIT: a deep learning framework for prediction of hERG-induced cardiotoxicity. *Bioinformatics*, 36(10):3049–3055, May 2020.

C. E. Shannon. A mathematical theory of communication. *The Bell System Technical Journal*, 27:379–423, 1948. URL <http://plan9.bell-labs.com/cm/ms/what/shannonday/shannon1948.pdf>.

E. Steinberg, K. Jung, J. A. Fries, C. K. Corbin, S. R. Pfohl, and N. H. Shah. Language models are an effective representation learning technique for electronic health record data. *Journal of Biomedical Informatics*, 113:103637, 2021.

J. Su, Y. Lu, S. Pan, A. Murtadha, B. Wen, and Y. Liu. Roformer: Enhanced transformer with rotary position embedding, 2021. URL <https://arxiv.org/abs/2104.09864>.

M. J. Van der Laan and J. M. Robins. *Unified methods for censored longitudinal data and causality*, volume 5. Springer, 2003.

A. Vaswani, N. Shazeer, N. Parmar, J. Uszkoreit, L. Jones, A. N. Gomez, L. u. Kaiser, and I. Polosukhin. Attention is all you need. In I. Guyon, U. V. Luxburg, S. Bengio, H. Wallach, R. Fergus, S. Vishwanathan, and R. Garnett, editors, *Advances in Neural Information Processing Systems*, volume 30. Curran Associates, Inc., 2017. URL <https://proceedings.neurips.cc/paper/2017/file/3f5ee243547dee91fbd053c1c4a845aa-Paper.pdf>.

Z. Wang and J. Sun. Survtrace: Transformers for survival analysis with competing events. *CoRR*, abs/2110.00855, 2021. URL <https://arxiv.org/abs/2110.00855>.

Y. Wen, M. F. Rahman, Y. Zhuang, M. Pokojovy, H. Xu, P. McCaffrey, A. Vo, E. Walser, S. Moen, and T. B. Tseng. Time-to-event modeling for hospital length of stay prediction for COVID-19 patients. *Mach Learn Appl*, 9:100365, Sep 2022.

W. C.-H. Wu, M.-Y. Yeh, and M.-S. Chen. Predicting winning price in real time bidding with censored data. In *Proceedings of the 21th ACM SIGKDD International Conference on Knowledge Discovery and Data Mining*, KDD ’15, page 1305–1314, New York, NY, USA, 2015. Association for Computing Machinery. ISBN 9781450336642. doi: 10.1145/2783258.2783276. URL <https://doi.org/10.1145/2783258.2783276>.

X. Zeng, S. L. Linwood, and C. Liu. Pretrained transformer framework on pediatric claims data for population specific tasks. *Scientific Reports*, 12(1):3651, Mar 2022. ISSN 2045-2322. doi: 10.1038/s41598-022-07545-1. URL <https://doi.org/10.1038/s41598-022-07545-1>.

Appendix A. Hyperparameter Search Grids

Hyperparameters	Values
Count Based Representation	
min_patients	100, 1000
ontology_expansion	false, true
Cox PH	
lambda	automatic
software_version	glmnet 4.1-6
DeepSurv	
dropout	0, 0.1
inner_layer_size	32, 128, 256, 512
learning_rate	10^{-3} , 10^{-4} , 10^{-5}
software_version	pycox 0.2.3
Random Survival Forests	
node_size	5, 15, 50, 100
min_time_bins	8, 16, 32
software_version	rfsrc 3.1.0
MOTOR	
dropout	0, 0.1
learning_rate	10^{-3} , 10^{-4} , 10^{-5}
num_time_bins	8, 16
survival_dim	256, 512
inner_dim	768
layers	6
max_sequence_length	16,384
vocabulary_size	65,536
software_version	piton d9d22c6

Table S1: Hyperparameter search grids of methods under comparison in our experiments. The software version for implementing each method is also shown.

Appendix B. Subsampling Bias

For our experiments, we use a simple subsampling strategy where we drop a fraction d of the censored examples in our dataset before modeling and evaluation. This causes a non-uniform scaling of the hazard rates. Let $H_i(t)$ be the hazard rate for a particular time t and let $\tilde{H}_i(t)$ be the hazard rate for a particular time t induced by our subsampling strategy. Equation 7 provides the ratio of $\tilde{H}_i(t)$ and $H_i(t)$. Proof 7 is the derivation of that equation.

$$\frac{\tilde{H}_i(t)}{H_i(t)} = \frac{1}{1 - d \mathbb{P}(C_i < T_i | C_i > t, T_i > t)} \quad (7)$$

Proof. The hazard in our original dataset before sampling is

$$\begin{aligned} H_i(t) &= \frac{\mathbb{P}(T_i = t)}{\mathbb{P}(T_i > t)} \\ &= \frac{\mathbb{P}(T_i = t) \mathbb{P}(C_i > t)}{\mathbb{P}(T_i > t) \mathbb{P}(C_i > t)} \\ &= \frac{\mathbb{P}(T_i = t, C_i > t)}{\mathbb{P}(T_i > t, C_i > t)} \quad \text{assume } C_i \perp\!\!\!\perp T_i \\ &= \frac{\mathbb{P}(T_i = t, C_i > t)}{\mathbb{P}(C_i < T_i, C_i > t, T_i > t) + \mathbb{P}(C_i \geq T_i, C_i > t, T_i > t)} \end{aligned}$$

The hazard in our dataset after sampling is

$$\begin{aligned} \tilde{H}_i(t) &= \frac{\mathbb{P}(T_i = t, C_i > t)}{(1 - d) \mathbb{P}(C_i < T_i, T_i > t, C_i > t) + \mathbb{P}(C_i \geq T_i, T_i > t, C_i > t)} \\ &= \frac{\mathbb{P}(T_i = t, C_i > t)}{((1 - d) \mathbb{P}(C_i < T_i | T_i > t, C_i > t) + \mathbb{P}(C_i \geq T_i | T_i > t, C_i > t)) \mathbb{P}(T_i > t, C_i > t)} \\ &= \frac{\mathbb{P}(T_i = t, C_i > t)}{((1 - d) \mathbb{P}(C_i < T_i | T_i > t, C_i > t) + (1 - \mathbb{P}(C_i < T_i | T_i > t, C_i > t))) \mathbb{P}(T_i > t, C_i > t)} \\ &= \frac{\mathbb{P}(T_i = t, C_i > t)}{(1 - d \mathbb{P}(C_i < T_i | T_i > t, C_i > t)) \mathbb{P}(T_i > t, C_i > t)} \\ &= \frac{H_i(t)}{1 - d \mathbb{P}(C_i < T_i | T_i > t, C_i > t)} \end{aligned}$$

Thus,

$$\frac{\tilde{H}_i(t)}{H_i(t)} = \frac{1}{1 - d \mathbb{P}(C_i < T_i | C_i > t, T_i > t)}$$

□

Appendix C. Confidence Intervals

Table S2: 95% confidence intervals of difference in time-dependent C statistic between MOTOR and the other methods on the full dataset. Higher numbers are considered better for this metric. Asterisks indicate statistically significant entries at $p = 0.05$. RSF = Random Survival Forest. MOTOR-WP = MOTOR Without Pretraining.

Method	Celiac	Heart Attack	Lupus	NAFLD	Pancreatic Cancer	Stroke
Cox PH	[-0.139, -0.086]*	[-0.143, -0.103]*	[-0.099, -0.060]*	[-0.142, -0.125]*	[-0.092, -0.049]*	[-0.104, -0.086]*
DeepSurv	[-0.122, -0.072]*	[-0.075, -0.045]*	[-0.078, -0.042]*	[-0.066, -0.053]*	[-0.075, -0.034]*	[-0.051, -0.037]*
RSF	[-0.093, -0.050]*	[-0.063, -0.033]*	[-0.081, -0.045]*	[-0.064, -0.051]*	[-0.060, -0.023]*	[-0.041, -0.028]*
MOTOR-WP	[-0.132, -0.079]*	[-0.110, -0.069]*	[-0.068, -0.026]*	[-0.044, -0.032]*	[-0.113, -0.063]*	[-0.050, -0.036]*
MOTOR	[0.000, 0.000]	[0.000, 0.000]	[0.000, 0.000]	[0.000, 0.000]	[0.000, 0.000]	[0.000, 0.000]

Table S3: 95% confidence intervals for the difference in ND calibration between MOTOR and the methods on the full dataset. Lower numbers are better for this metric. Asterisks indicate statistically significant entries at $p = 0.05$. RSF = Random Survival Forest. MOTOR-WP = Motor Without Pretraining.

Method	Celiac	Heart Attack	Lupus	NAFLD	Pancreatic Cancer	Stroke
Cox PH	[0.011, 0.239]*	[0.068, 0.321]*	[0.173, 0.522]*	[0.072, 0.135]*	[-0.094, 0.192]	[-0.029, 0.030]
DeepSurv	[-0.081, 0.088]	[-0.028, 0.162]	[-0.035, 0.155]	[2.592, 3.267]*	[-0.120, 0.193]	[-0.037, 0.042]
RSF	[0.120, 0.426]*	[0.049, 0.323]*	[-0.050, 0.131]	[0.040, 0.108]*	[0.099, 0.490]*	[0.043, 0.125]*
MOTOR-WP	[2.556, 10.321]*	[2.073, 10.747]*	[10.942, 51.232]*	[0.023, 0.099]*	[2.859, 19.977]*	[-0.001, 0.156]
MOTOR	[0.000, 0.000]	[0.000, 0.000]	[0.000, 0.000]	[0.000, 0.000]	[0.000, 0.000]	[0.000, 0.000]

Table S4: 95% confidence intervals for the difference in MOTOR’s time-dependent C statistic when the pretraining task is changed. We evaluate both a “next code” baseline as well as our proposed time-to-event objective. Note that these experiments are done with full fine-tuning of the entire model. Asterisks indicate statistically significant entries at $p = 0.05$.

Objective	Celiac	Heart Attack	Lupus	NAFLD	Pancreatic Cancer	Stroke
Next Code	[-0.043, -0.007]*	[-0.031, -0.007]*	[-0.029, -0.004]*	[-0.008, 0.000]	[-0.018, 0.014]	[-0.022, -0.012]*
Time-to-Event	[0.000, 0.000]	[0.000, 0.000]	[0.000, 0.000]	[0.000, 0.000]	[0.000, 0.000]	[0.000, 0.000]

Table S5: 95% confidence intervals for the difference in time-dependent C statistic between pretraining on 100% of the training data vs more limited subsets. Asterisks indicate statistically significant entries at $p = 0.05$.

% Used	Celiac	Heart Attack	Lupus	NAFLD	Pancreatic Cancer	Stroke
5%	[-0.130, -0.084]*	[-0.052, -0.028]*	[-0.132, -0.089]*	[-0.099, -0.084]*	[-0.058, -0.022]*	[-0.057, -0.044]*
10%	[-0.109, -0.066]*	[-0.046, -0.023]*	[-0.124, -0.081]*	[-0.080, -0.067]*	[-0.052, -0.016]*	[-0.053, -0.040]*
25%	[-0.078, -0.041]*	[-0.041, -0.020]*	[-0.081, -0.044]*	[-0.066, -0.054]*	[-0.041, -0.014]*	[-0.047, -0.035]*
100%	[0.000, 0.000]	[0.000, 0.000]	[0.000, 0.000]	[0.000, 0.000]	[0.000, 0.000]	[0.000, 0.000]

Table S6: 95% confidence intervals for the difference in time-dependent C statistic between fine-tuning on 100% of the training data vs subsets of the data. Asterisks indicate statistically significant entries at $p = 0.05$.

% Used	Celiac	Heart Attack	Lupus	NAFLD	Pancreatic Cancer	Stroke
5%	[-0.029, -0.005]*	[-0.010, -0.001]*	[-0.018, -0.003]*	[-0.010, -0.007]*	[-0.025, -0.004]*	[-0.009, -0.004]*
10%	[-0.033, -0.008]*	[-0.015, -0.004]*	[-0.012, 0.000]	[-0.006, -0.004]*	[-0.018, -0.003]*	[-0.008, -0.004]*
25%	[-0.018, -0.005]*	[-0.007, -0.000]*	[-0.010, 0.000]	[-0.005, -0.003]*	[-0.010, -0.002]*	[-0.006, -0.004]*
100%	[0.000, 0.000]	[0.000, 0.000]	[0.000, 0.000]	[0.000, 0.000]	[0.000, 0.000]	[0.000, 0.000]